

Triangular I_{mn} Integral and Application for Computation of Stability Coefficients of Arbitrary Cross Section

Toufik Yahiaoui* and Toufik Zebbiche*

Keywords : Double integral, Green transformation, Triangular element, Mesh generation, Cubic spline interpolation, Geometrics characteristics, Arbitrary cross sections, Simpson quadrature, Stability coefficients, Non symmetrical Airfoils, Jacobean, Finite Elements Method, Elementary stiffness matrix, Elementary mass matrix.

ABSTRACT

The aim of this work consists of developing a numerical computation program allowing to evaluate the integrals I_{mn} of high order in the surface of any triangle given by the coordinates of these three nodes and to apply for the elementary stiffness and mass matrices of higher order finite elements as well as for the calculation of the stability coefficients of straight sections of arbitrary geometries such as airfoils and other sections interesting in engineering field. The calculation of I_{mn} is performed according to the three segments of the triangle boundary in a counterclockwise direction by the application of the Green's transformation. The integral I_{mn} is therefore presented by a numerical integration of three functions by the use of Simpson's quadrature. Cubic spline interpolation is used to determine an analytical shape of the airfoils equation for the upper and the lower surfaces as the latter are given by a tabulated values. The discretization of the section by the generation of a triangular mesh with a single observer is presented to compute the I_{mn} of the section. The calculation of the stabilities coefficients with respect to the central axes is made using the principle of parallel axes. The calculation of high order I_{mn} for the triangular reference element valid for the generation of the new finite elements at the level of elementary calculation of the stiffness and mass matrices is also presented.

*Paper Received March, 2021. Revised May, 2021. Accepted August, 2021. Author for Correspondence: Toufik Zebbiche.
Email : z_toufik270169@yahoo.fr*

**Professor, Institute of Aeronautics and Space Studies, University of Blida 1, BP 270 Blida 09000, Algeria.*

INTRODUCTION

The triangular surface plays a very important role for the decomposition of any surfaces in order to obtain a simple elementary section. The return of the triangular section to the original mother section is done by the generation of triangular mesh either by a single observer as presented in this study or by an arbitrary distribution in these two coordinate system directions. Then the basis of calculation for any section is the triangular section defined by the coordinates of these three nodes. The calculation of the triangular integral I_{mn} in any triangle is also of a very important mathematical and engineering interest given the direct applications in the *FEM* for the evaluation of the elementary stiffness and mass matrices of the triangular elements of order bred with multiple nodes with multiple *DOFs*. Other very interesting applications for example for the evaluation of the stabilities coefficients of unspecified sections of complex and arbitrary geometries. Then our integral is a clean and regular double integral. The function under the integral sign is the term of the limited expansion of any two-variable function.

Reddy (2007) and Iron and Ahmed (1990) evaluate the integrals I_{mn} in order to calculate the geometrical characteristics in a triangle defined by the coordinates of these three nodes by the analytical method. Zebbiche et al. (2014) represents a direct calculation of the integral I_{mn} for evaluation of the geometric characteristics of complex sections and to apply for any airfoils geometries. Megson (2005, 2007) present the formulas for calculating the stability coefficients of the usual sections known in the literature. These coefficients are evaluated on the basis of our integrals I_{mn} when $m+n=3$.

The goal of this present work consists in developing a numerical computation program allowing to evaluate the integrals I_{mn} of high order when $m+n$ is greater than or equal to 3 in the area of any triangle given by the coordinates of these three nodes. The applications presented will be set for evaluating the elementary stiffness and mass matrices of higher order finite elements, as well as for the

calculation of the stability coefficients of cross sections of arbitrary geometries, such as airfoils, and other general and arbitrary sections interested in the field of engineering. Green's transform is used to transform the surface integral to the curvilinear boundary calculus of the three segments counter clockwise. The integral I_{mn} is therefore presented by a numerical integration of three functions by the use of Simpson's quadrature. As the boundary of the airfoils geometries is given by tabulated values, the cubic spline interpolation is therefore used and numerically programmed to determine an analytical shape for the airfoils equation for the upper surface of extrados and the lower surface of the intrados. The discretization of the section is made by the generation of a structured triangular mesh with only one internal observer to evaluate the computation of I_{mn} of the section. The calculation of the stabilities coefficients with respect to the central axes is made using the principle of parallal axes. The computation of the I_{mn} of high order for the triangular reference element valid for the generation of new finite elements at the level of elementary computation of the stiffness and mass matrices is also presented.

MATHEMATICAL FORMULATION

The interested I_{mn} integral in our work is presented by the following Eq. (1) in the triangular geometry shown in the figure 1 (Reddy, 2007), (Irons and Ahmed, 1990) and (Kardestuncer et al., 2010).

The integral (1) is a type of proper double integral of a regular function having the term of limited expansion of any continuous function. The values (n, m) are any positive integers.

$$I_{mn} = \int_{\Delta} x^m y^n dA \tag{1}$$

To evaluate the double integral I_{mn} we use Green's transformation to go from a surface integral to a curvilinear integral along the boundary contours in a counterclockwise direction. Then according to Piskounov (1987) and Lofficial and Tarré (2006), we can demonstrate the following formula:

$$\iint_S \left[\frac{\partial G}{\partial x} - \frac{\partial F}{\partial y} \right] dx dy = \oint [F dx + G dy] \tag{2}$$

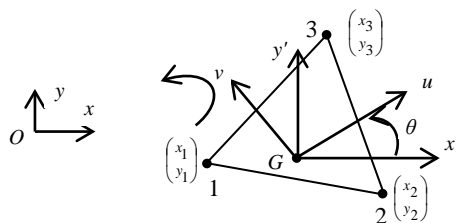


Fig. 1 Triangular element with three nodes.

To obtain the result, we can arbitrarily choose the function F or G . For example we get $G=0$, then:

$$\frac{\partial F}{\partial y} = x^m y^n \tag{3}$$

The integration of the relation (3) to obtain the function F gives:

$$F = -\frac{1}{n+1} x^m y^{n+1} \tag{4}$$

Replace Eq. (4) in (3), we get:

$$I_{mn} = \int_{\Delta} x^m y^n dx dy = -\oint \frac{x^m y^{n+1}}{n+1} dx \tag{5}$$

Integration along the closed contour of the triangle along the trigonometric direction gives

$$I_{mn} = - \left[\int_{x_1}^{x_2} \frac{x^m y^{n+1}}{n+1} dx + \int_{x_2}^{x_3} \frac{x^m y^{n+1}}{n+1} dx + \int_{x_3}^{x_1} \frac{x^m y^{n+1}}{n+1} dx \right] \tag{6}$$

In the relation (6) and compared to the relation (5), we changed the order of integration to remove the negative sign.

Axes Translation

With respect to the central axes Gx' and Gy' as shown in figure 1, we can define the integral I'_{mn} by the following relation:

$$I'_{mn} = \int_{\Delta} x'^m y'^n dA \tag{7}$$

The translation of the axes between the reference mark for the definition of the surface xOy and the reference mark for the central axes $x'Gy'$ according to the figure 1 is given by:

$$x' = x - x_G \tag{8}$$

$$y' = y - y_G \tag{9}$$

Replace (8) and (9) in (7), then transform (7) into a curvilinear integral according to (6), we get:

$$I'_{mn} = \left[\int_{x_1}^{x_2} \frac{(x-x_G)^m (y-y_G)^{n+1}}{n+1} dx + \int_{x_2}^{x_3} \frac{(x-x_G)^m (y-y_G)^{n+1}}{n+1} dx + \int_{x_3}^{x_1} \frac{(x-x_G)^m (y-y_G)^{n+1}}{n+1} dx \right] \tag{10}$$

For any triangle given by the coordinates of these tri nodes of its end, the coordinates (x_G, y_G) are given by Redy (2007), Irons and Ahmed (1990) and Zebbiche et al. (2014):

$$x_G = \frac{1}{3}(x_1 + x_2 + x_3) \tag{11}$$

$$y_G = \frac{1}{3}(y_1 + y_2 + y_3) \tag{12}$$

Rotation of Central Axes

When the central axes rotating by an angle θ around point G as shown in the figure 1, we obtain the

integrals I_{mn}^θ with respect to the axes Gu and Gv . When $\theta=0$, the axes Gu and Gx will be the same. The same goes for the Gv and Gy axes. In this case, we will not have a rotation.

The relations between the coordinates of a point with respect to the $Gx'y'$ and Guv coordinate systems are given by:

$$u = x' \cos \theta + y' \sin \theta \tag{13}$$

$$v = -x' \sin \theta + y' \cos \theta \tag{14}$$

The results presented by (13) and (14) can be demonstrated using the relation of Chasles (Eiden, 2009) and (Mercier, 2014).

With respect to the axes Gu and Gv , we can define the integral I_{mn}^θ by the following relation:

$$I_{mn}^\theta = \int_{\Delta} u^m v^n dA \tag{15}$$

Before developing the relation (15), we need the following transformation (Lehning, 2017):

$$(a-b)^n = \sum_{k=0}^{k=n} (-1)^{n-k} C_n^k a^{n-k} b^k \tag{16}$$

With

$$C_n^k = \frac{n!}{k!(n-k)!} \tag{17}$$

And

$$k! = k(k-1)(k-2)\dots \times 3 \times 2 \times 1 \tag{18}$$

$$0! = 1 \tag{19}$$

We replace expressions (13) and (14) in (15) then using the relation (16) we get, after rearrangement, the following result:

$$I_{mn}^\theta = \sum_{i=0}^{i=m} \sum_{j=0}^{j=n} \left[(-1)^{m+n-j} C_m^i C_n^j \cos^{m+n-i-j} \theta \sin^{i+j} \theta \times I_{(m-i+j)(n+i-j)}^\theta \right] \tag{20}$$

Once the calculation of the I_{mn}^θ is done, one can easily and analytically only determine the integrals I_{mn}^θ using the relation (20). In this relation all the integrals of I_{mn}^θ varying m and n such that $m+n$ invariable (given) enters for the evaluation of I_{mn}^θ .

The integral I_{mn}^θ is a trigonometric function of the variable angle θ . It is very interesting to determine the angles Ω_1 corresponding to the maximum and the minimum values of I_{mn}^θ . These values corresponding to the axes which are called by principal axes of I_{mn}^θ and the values of I_{mn}^θ corresponding to these directions are called by principal I_{mn}^θ .

The search for these directions is done by calculating the root of the derivative of the function I_{mn}^θ given by (20) with respect to the angle θ . We set the derivative of I_{mn}^θ by $f(\theta)$. So we get:

$$\frac{d(I_{mn}^\theta)}{d\theta} = 0 = f_{mn}(\theta) = \sum_{i=0}^{i=m} \sum_{j=0}^{j=n} \left[(-1)^{m+n-j} C_m^i C_n^j I_{(m-i+j)(n+i-j)}^\theta \times \left[\cos^{m+n-i-j} \theta \sin^{i+j} \theta \times (i+j - (m+n) \sin^2 \theta) \right] \right] \tag{21}$$

We are interested in the $I_{mn}^\theta(\theta)$ in the interval $[0, 2\pi]$. Equation (21) is of a transcendent nonlinear type. The search for the roots of (21) is done by the dichotomy algorithm (Démidivitch and Maron, 1987) and (Raltson and Rabinowitz, 1985) in the interval $[0, 2\pi]$.

CALCULATION PROCEDURE OF I_{mn} and I_{mn}^θ

Consider the integration along the line connecting points 1 and 2 according to the figure 1. Regarding relation (6), we set:

$$J_{12} = - \int_{x_1}^{x_2} \frac{x^m y^{n+1}}{n+1} dx \tag{22}$$

The analytical equation of the line connecting the points 1 and 2 is written:

$$y = \alpha_{12} x + \gamma_{12} \tag{23}$$

With

$$\alpha_{12} = \frac{y_2 - y_1}{x_2 - x_1} \tag{24}$$

$$\gamma_{12} = y_1 - \frac{y_2 - y_1}{x_2 - x_1} x_1 \tag{25}$$

Then the integral J_{12} becomes:

$$J_{12} = - \frac{1}{n+1} \int_{x_1}^{x_2} x^m (\alpha_{12} x + \gamma_{12})^{n+1} dx \tag{26}$$

We set the following change of variable:

$$x = a z + b \tag{27}$$

For $x=x_1$ we have $z=0$ and for $x=x_2$ we have $z=1$. So we find the relation:

$$x = (x_2 - x_1) z + x_1 \tag{28}$$

We put

$$x_{12} = x_1 - x_2 \tag{29}$$

$$y_{12} = y_1 - y_2 \tag{30}$$

By replacing the expressions (23), (24), (25) in the relation (26), we will have after rearrangement the following result:

$$J_{12} = \frac{1}{n+1} x_{12} \int_0^1 [-x_{12} z + x_1]^m [-y_{12} z + y_1]^{n+1} dz \tag{31}$$

We can easily deduce the integrals along the lines respectively connecting the points 2 and 3 as well as the point 3 and 1. We set J_{23} the integral according to the points 2 and 3 and by J_{31} the integral according to

the points 3 and 1. To deduce the result of J_{23} from J_{12} , it suffices to replace the index 1 by 2 and the index 2 by 3, or x_1 by x_2 , y_1 by y_2 , x_2 by x_3 and y_2 by y_3 . We put in this case:

$$x_{23} = x_2 - x_3, \quad x_{31} = x_3 - x_1 \quad (32)$$

$$y_{23} = y_2 - y_3, \quad y_{31} = y_3 - y_1 \quad (33)$$

Then

$$J_{23} = \frac{1}{n+1} x_{23} \int_0^1 [-x_{23}z + x_2]^m [-y_{23}z + y_2]^{n+1} dz \quad (34)$$

and

$$J_{31} = \frac{1}{n+1} x_{31} \int_0^1 [-x_{31}z + x_3]^m [-y_{31}z + y_3]^{n+1} dz \quad (35)$$

Finally, we get:

$$I_{mn} = J_{12} + J_{23} + J_{31} \quad (36)$$

For the relation (10), by making the same change of variable (27), we end up with the following result

$$I'_{mn} = J'_{12} + J'_{23} + J'_{31} \quad (37)$$

with

$$J'_{12} = \frac{x_{12}}{n+1} \int_0^1 [-x_{12}z + x_1 - x_G]^m [-y_{12}z + y_1 - y_G]^{n+1} dz \quad (38)$$

$$J'_{23} = \frac{x_{23}}{n+1} \int_0^1 [-x_{23}z + x_2 - x_G]^m [-y_{23}z + y_2 - y_G]^{n+1} dz \quad (39)$$

$$J'_{31} = \frac{x_{31}}{n+1} \int_0^1 [-x_{31}z + x_3 - x_G]^m [-y_{31}z + y_3 - y_G]^{n+1} dz \quad (40)$$

ANALYTICAL CALCULATION OF I_{mn} and I'_{mn}

A simple procedure for calculating the integrals I_{mn} and I'_{mn} .

Analytical Calculation of I_{mn}

By using the relation (16) in the Eqs. (31), (34) and (35), we will have after integration and rearrangement respectively the following results:

$$J_{12} = \frac{1}{n+1} \sum_{i=0}^{i=m} \sum_{j=0}^{j=n+1} \frac{(-1)^{m+n-i-j} C_m^i C_{n+1}^j}{m+n+2-i-j} x_{12}^{m+1-i} x_1^i y_{12}^{n+1-j} y_1^j \quad (41)$$

$$J_{23} = \frac{1}{n+1} \sum_{i=0}^{i=m} \sum_{j=0}^{j=n+1} \frac{(-1)^{m+n-i-j} C_m^i C_{n+1}^j}{m+n+2-i-j} x_{23}^{m+1-i} x_2^i y_{23}^{n+1-j} y_2^j \quad (42)$$

$$J_{31} = \frac{1}{n+1} \sum_{i=0}^{i=m} \sum_{j=0}^{j=n+1} \frac{(-1)^{m+n-i-j} C_m^i C_{n+1}^j}{m+n+2-i-j} x_{31}^{m+1-i} x_3^i y_{31}^{n+1-j} y_3^j \quad (43)$$

With x_{12} , y_{12} , x_{23} , y_{23} , x_{31} and y_{31} are given by the relations (29), (30), (32) and (33).

Analytical Calculation of I'_{mn}

Replacing again the relation (16) in the relations (38), (39) and (40), we will have after integration and rearrangement respectively the following results:

$$J'_{12} = \frac{1}{n+1} \sum_{i=0}^{i=m} \sum_{j=0}^{j=n+1} \left[\frac{(-1)^{m+n-i-j} C_m^i C_{n+1}^j}{m+n+2-i-j} x_{12}^{m+1-i} (x_1 - x_G)^i \times y_{12}^{n+1-j} (y_1 - y_G)^j \right] \quad (44)$$

$$J'_{23} = \frac{1}{n+1} \sum_{i=0}^{i=m} \sum_{j=0}^{j=n+1} \left[\frac{(-1)^{m+n-i-j} C_m^i C_{n+1}^j}{m+n+2-i-j} x_{23}^{m+1-i} (x_2 - x_G)^i \times y_{23}^{n+1-j} (y_2 - y_G)^j \right] \quad (45)$$

$$J'_{31} = \frac{1}{n+1} \sum_{i=0}^{i=m} \sum_{j=0}^{j=n+1} \left[\frac{(-1)^{m+n-i-j} C_m^i C_{n+1}^j}{m+n+2-i-j} x_{31}^{m+1-i} (x_3 - x_G)^i \times y_{31}^{n+1-j} (y_3 - y_G)^j \right] \quad (46)$$

With x_{12} , y_{12} , x_{23} , y_{23} , x_{31} , y_{31} , x_G and y_G are given by the relations (29), (30), (32), (33), 11 and 12.

NUMERICAL CALCULATION OF I_{mn} AND I'_{mn}

Among several numerical calculation methods, the integrals (31), (35) and (36) as well as the integrals (38), (39) and (40) can be evaluated numerically by the use of the Simpson's quadrature (Démidovitch and Maron, 1987) and (Raltson and Rabinowitz, 1985).

For $m+n=0$, $m+n=1$ and $m+n=2$, i.e. I_{00} , I_{10} , I_{01} , I_{20} , I_{11} and I_{02} are presented in the Refs (Reddyn 2007), (Irons and Ahmed, 1990) and (Zebbiche, Boun-jad and Allali, 2014) for the purpose of calculating the geometric characteristics of straight sections and application to airfoils. The aim of our present work is to evaluate the integrals (36) and (37) of high order when $m+n>2$ and applications to the mathematical and engineering calculations illustrated in the following paragraph.

APPLICATIONS

Our application is made to evaluate the integrals I_{mn} and I'_{mn} when $m+n=3$ up to 10 for finite element application and to calculate the stability coefficients with respect to the definition axes and the central axes of the section for them usual and other sections of airfoils.

Stabilities Coefficients

By definition, for any section according to the figure 2 and with respect to the reference mark axes Ox and Oy of definition, the stability coefficients can

be calculated by the following formulas (Megson, 2005, 2007):

$$\beta_y = \int_A x(x^2 + y^2) dA = I_{30} + I_{12} \quad (47)$$

$$\beta_x = \int_A y(x^2 + y^2) dA = I_{21} + I_{03} \quad (48)$$

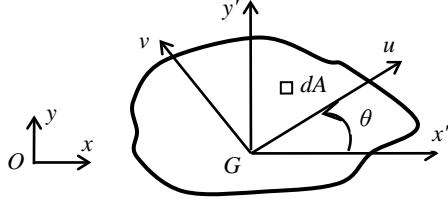


Fig. 2 Translation and rotation of axes

With respect to the central axes reference mark, we can evaluate $\beta_{x'}$ and $\beta_{y'}$ by the following relations:

$$\beta_{y'} = \int_A x'(x'^2 + y'^2) dA = I'_{30} + I'_{12} \quad (49)$$

$$\beta_{x'} = \int_A y'(x'^2 + y'^2) dA = I'_{21} + I'_{03} \quad (50)$$

The calculation of the stabilities coefficients with respect to the axes of rotation can be extended in order to determine the maximum value and the minimum value of these coefficients as well as the direction of the axes carrying these values. With respect to the axes Gu and Gv obtained by rotating through an angle θ of the central axes Gx' and Gy' , the coefficients β_u^θ and β_v^θ can be determined by the following relations:

$$\beta_u^\theta = I'_{21} + I'_{03} \quad (51)$$

$$\beta_v^\theta = I'_{30} + I'_{12} \quad (52)$$

Then the coefficients $\beta_x, \beta_y, \beta_{x'}, \beta_{y'}, \beta_u^\theta$ and β_v^θ are special cases of the integrals I_{mn}, I'_{mn} and I''_{mn} when $m+n=3$.

We can show that the coefficients β_u^θ and β_v^θ are related by the following relation:

$$\beta_v^\theta = \beta_u^\theta \left(\theta + \frac{\pi}{2} \right) \quad (53)$$

The calculation can be extended by the numerical evaluation of the moments of the following stability coefficients. Then compared to the reference xOy , they are defined by (Megson, 2005, 2007):

$$\gamma_y = \int_A x^2(x^2 + y^2) dA = I_{40} + I_{22} \quad (54)$$

$$\gamma_{xy} = \int_A xy(x^2 + y^2) dA = I_{31} + I_{13} \quad (55)$$

$$\gamma_x = \int_A y^2(x^2 + y^2) dA = I_{04} + I_{22} \quad (56)$$

And with respect to the $x'Gy'$ benchmark, they are defined by:

$$\gamma_{y'} = \int_A x'^2(x'^2 + y'^2) dA = I'_{40} + I'_{22} \quad (57)$$

$$\gamma_{x'y'} = \int_A x'y'(x'^2 + y'^2) dA = I'_{31} + I'_{13} \quad (58)$$

$$\gamma_{x'} = \int_A y'^2(x'^2 + y'^2) dA = I'_{04} + I'_{22} \quad (59)$$

With respect to the axes of rotation of an angle θ , these coefficients can be calculated by:

$$\gamma_u^\theta = I'_{40} + I'_{22} \quad (60)$$

$$\gamma_{uv}^\theta = I'_{13} + I'_{31} \quad (61)$$

$$\gamma_v^\theta = I'_{04} + I'_{22} \quad (62)$$

FEM Applications

The calculation of the elementary stiffness and mass matrices of higher order finite elements as well as the calculation of the equivalent force vector of distributed loadings can be considered as a good application of the use of the integral I_{mn} of our study. Then according to (Irons, Ahmed, 1990) and (Imbert, 1991), the calculation of the elementary stiffness and mass matrices of the finite elements as well as the equivalent force vector can be evaluated respectively by the following formulas:

$$[K] = \int_V [B]^T [E] [B] dV \quad (63)$$

$$[M] = \int_V \rho [N]^T [N] dV \quad (64)$$

$$\{F\} = \int_V [N]^T f(x, y) dV \quad (65)$$

For the stiffness matrix, the elements K_{ij} ($i=1, 2, \dots, n$), ($j=1, 2, \dots, n$) can be calculated by the following formula (Irons, Ahmed, 1990) and (Imbert, 1991).

$$K_{ij} = t \sum_{p=1}^{p=3} \sum_{q=1}^{q=3} E_{pq} \int_{\Delta} B_{pi} B_{qj} dA \quad (66)$$

Likewise, the elements of the mass matrix can be determined by the contribution of the following integral:

$$M_{ij} = \int_{\Delta} N_i N_j dA \quad (67)$$

For the relation (65), we can write:

$$F_i = t \int_{\Delta} N_i f(x, y) dA \quad (68)$$

In the Eq. (66), the elements of matrix $[B]$ can be evaluated by (Irons, Ahmed, 1990) and (Imbert, 1991):

$$[B] = \begin{bmatrix} \frac{\partial}{\partial x} & 0 \\ 0 & \frac{\partial}{\partial y} \\ \frac{\partial}{\partial y} & \frac{\partial}{\partial x} \end{bmatrix} [N] \quad (69)$$

Then, the matrix $[B]$ represents the derivative of the interpolation functions. As results, the calculation of the integrals (66), (67) and (68) is directly related with the interpolation functions.

$$[N(x, y)] = [g(x, y)] [H]^{-1} \quad (70)$$

With

$$[g(x, y)] = \begin{bmatrix} 1 & x & y & \dots & x^m y^n & 0 & 0 & 0 & \dots & 0 \\ 0 & 0 & 0 & \dots & 0 & 1 & x & y & \dots & x^m y^n \end{bmatrix} \quad (71)$$

For the two-dimensional elasticity, it is generally used to study the shear of thin plates. In this case each node has at least two *DOFs* which are (u, v) in the xGy plane. These two *DOFs* are in a sense of physical *DOFs*. In some cases we can extend and use higher order mathematical *DOFs* such as higher order derivatives by x and y of the functions u and v to minimize the number of nodes in the element.

The distribution of the nodes in an element is done in this general case between vertices, edges and surface. Then, there are 3 different positions of the nodes in an element. So in a triangular element we have 3 vertices and in a quadrilateral element we have 4 vertices. Regarding the nodes of the edges, it is necessary to multiply the number of nodes of the edges by 3 for the triangular element to have symmetry. The nodes of the surface must be symmetrical about the center of gravity of the element. For example if we have a number N nodes, and we want to share them and distribute them in a triangular element, we must remove 3 nodes from the 3 vertices then place a certain number of nodes following each edge and multiply it by 3 following of 3 edges and the rest will be placed in the surface of the element and which will be a multiple of 3 or 1 remaining node. If there is still a node, this situation exists and it will be placed at the level of the center of gravity of the triangular element. If the number of nodes remaining equal to 2 after distribution, this configuration will not be considered since it will not have symmetry. If the number of nodes remains equal to zero, in this case we will have a node at the level of the center of gravity.

Several possibilities of the location of the nodes for a given total number of nodes.

The approximation of the displacement functions $u(x, y)$ and $v(x, y)$, i.e. the number of term $x^i y^j$ of Pascal's triangle is done on the basis of the number of nodes, exactly is done on the number of total *DOF* which will be divided equally into 2 dimensions.

Finite elements containing 3, 6, 10, 15, 21, 28, 36, ..., $(i+1)(i+2)/2$ nodes with i positive integer are called complete elements. Apart from these numbers, the finite elements said to be incomplete, since the terms of the same power will not all be present in the approximation of the displacement functions. To know if we have complete element or not for a certain number of nodes n , the following number must be a positive integer

$$i = \frac{-3 + \sqrt{8n+1}}{2} \quad n \geq 3 \quad (72)$$

The number i in the relation (72) represents the greatest power of the terms $x^m y^n$ with $m+n=i$ involved in the approximation of the displacement functions.

If i in the relation (72) is not an integer, we therefore calculate the number j by the following relation:

$$j = n - \frac{(\text{Int}(i) + 1)(\text{Int}(i) + 2)}{2} \quad (73)$$

This number represents the number of terms $x^m y^n$ ($m+n=i+1$) involved in the approximation of the displacement functions. With $\text{Int}(i)$: represents the integer part of the number i given by (72) which is not an integer in this case.

The choice of the j terms of $x^m y^n$ ($m+n=i+1$) among all the terms of the power $i+1$ must respect the symmetry between the directions x and y . Then several possibilities of choosing the approximation of the functions $u(x, y)$ and $v(x, y)$ can be taken into account. For example $n=56$, we will have $\text{Int}(i)=9$ and $j=1$. Then as a first result, the element containing 56 nodes is not a complete element and in the approximation of the functions $u(x, y)$ and $v(x, y)$ we will have a term $x^m y^n$ having a power $m+n=10$ to choose from among the 10 existing terms in Pascal's triangle. As the number of the terms to the power of 10 is equal to 11, we can choose the last term $x^5 y^5$ in the approximations of the functions $u(x, y)$ and $v(x, y)$ to have a symmetry. We can even choose the last term as being the two terms grouped together in a single constant by $(x^6 y^4 + x^4 y^6)$, or $(x^7 y^3 + x^3 y^7)$, or $(x^8 y^2 + x^2 y^8)$, or $(x^9 y + x y^9)$ or $(x^{10} + y^{10})$. The terms $x^m y^n$ whose $m+n \leq 9$ are all present in the approximations of the functions $u(x, y)$ and $v(x, y)$.

For the calculation of I_{mn} in the element, only the nodes of the vertices involved in the calculation. From this presentation, we notice that the terms $x^m y^n$ intervene extensively in the evaluation of integrals (66), (67) and (68).

MESH GENERATION

To evaluate the integrals (6) and (10) in any section, it is necessary to divide the section into small surfaces of triangular geometries linked all the points of the boundary by an internal common point of the section (a single observer) as represented by the figure 3. The internal point is chosen arbitrarily under the condition that it must be visible by all the points of the boundary (Lofficail and Tarré, 2006) and (Eiden, 2009). The coordinates of the boundary points are defined compared to the reference mark of the definition of the section. The numbering of the nodes of the section is done in the anti-clockwise direction. The number of points on the boundary is equal to N in addition to the internal point. Hence the total number of points is equal to $N+1$. Therefore, the number of triangles obtained is equal to N .

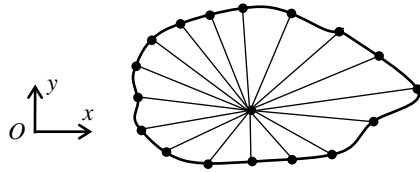


Fig. 3 Generation of triangular mesh with the boundary of the section and a single internal observer.

For the sections defined by tabulated values, cubic spline interpolation was used to determine an analytical expression at the boundary of the section (Raltson and Rabinowitz, 1985) and (Suenaga and Sukai, 2001). These sections can be found for example for wing airfoils, where their upper and lower edges are defined by tabulated values (Abbott and Duenhoff, 1959), (UIUC applied Aerodynamics Group, 2020) and (Ladson and Brooks, 1975). Among the set of airfoils, consider the RAE 2822 airfoils shown in the figure 4, whose tabulated points shown in the table 1 present the points of the geometry of its boundary. The number of the discretization points used for the evaluation of I_{mn} is different, or greater than that giving the geometry of the section.

Table 1: Defining points of the surface of the airfoil RAE 2822.

N	x/C (%)	$(y/C)_{Extrados}$ (%)	$(y/C)_{Intrados}$ (%)
01	0.0000	0.0000	0.0000
02	0.0602	0.3165	-0.3160
03	0.2408	0.6306	-0.6308
04	0.5412	0.9416	-0.9443
05	0.9607	1.2480	-1.2559
06	1.4984	1.5489	-1.5649
07	2.1530	1.8441	-1.8707
08	2.9228	2.1348	-2.1722
09	3.8060	2.4219	-2.4685
10	4.8005	2.7062	-2.7586
11	5.9039	2.9874	-3.0416
12	7.1136	3.2644	-3.3170
13	8.4265	3.5360	-3.5843
14	9.8396	3.8011	-3.8431
15	11.3495	4.0585	-4.0929
16	12.9524	4.3071	-4.3326
17	14.6447	4.5457	-4.5610
18	16.4221	4.7729	-4.7773
19	18.2803	4.9874	-4.9805
20	20.2150	5.1885	-5.1694
21	22.2215	5.3753	-5.3427
22	24.2949	5.5470	-5.4994
23	26.4302	5.7026	-5.6376
24	28.6222	5.8414	-5.7547
25	30.8658	5.9629	-5.8459
26	33.1555	6.0660	-5.9046
27	35.4858	6.1497	-5.9236
28	37.8510	6.2133	-5.8974
29	40.2455	6.2562	-5.8224
30	42.6635	6.2779	-5.6979
31	45.0991	6.2774	-5.5257
32	47.5466	6.2530	-5.3099
33	50.0000	6.2029	-5.0563
34	52.4534	6.1254	-4.7719
35	54.9009	6.0194	-4.4642

36	57.3365	5.8845	-4.1397
37	59.7545	5.7218	-3.8043
38	62.1490	5.5344	-3.4631
39	64.5142	5.3258	-3.1207
40	66.8445	5.0993	-2.7814
41	69.1342	4.8575	-2.4495
42	71.3778	4.6029	-2.1289
43	73.5698	4.3377	-1.8232
44	75.7051	4.0641	-1.5357
45	77.7785	3.7847	-1.2690
46	79.7850	3.5017	-1.0244
47	81.7197	3.2176	-0.8027
48	83.5779	2.9347	-0.6048
49	85.3553	2.6554	-0.4314
50	87.0476	2.3817	-0.2829
51	88.6505	2.1153	-0.1592
52	90.1604	1.8580	-0.0600
53	91.5735	1.6113	0.0157
54	92.8864	1.3769	0.0694
55	94.0961	1.1562	0.1033
56	95.1995	0.9508	0.1197
57	96.1940	0.7622	0.1212
58	97.0772	0.5915	0.1112
59	97.8470	0.4401	0.0935
60	98.5016	0.3092	0.0719
61	99.0393	0.2001	0.0497
62	99.4588	0.1137	0.0296
63	99.7592	0.0510	0.0137
64	99.9398	0.0128	0.0035
65	100.0000	0.0000	0.0000

The RAE 2822 airfoil along the boundary presented in the table 3 is illustrated in the figure 4. It is a non-symmetrical airfoil.



Fig. 4 Airfoil RAE 2822

RESULTS AND COMMENTS

Triangular Element of Reference

In the *FEM* applications, it is sometimes very useful to determine the elementary stiffness and the mass matrixes of the universal triangular and square finite elements of reference as shown in figures 5 and 6. For any triangular or quadrilateral finite element, it is sufficient that to make the change of variable of coordinates in going from the real geometry towards the geometry of reference by multiplying the integrals of $[K]^e$ and $[M]^e$ only by the Jacobean (Reddy, 2007) and (Imbert, 1991).

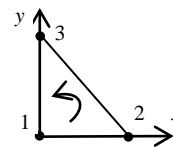


Fig. 5 Triangulaire element of reference.

For this element we have $(x_1, y_1)=(0, 0)$, $(x_2, y_2)=(1, 0)$ and $(x_3, y_3)=(0, 1)$.

Table 2 presents the results of I_{mn} and I'_{mn} for the triangular element of reference according to the figure 5 when $m+n=0$ up to 10. An integral I_{mn} when $m+n=10$ intervenes in the calculation of the interpolations functions and their derivatives of 2D finite elements when the number of *DOF* reaches 56 nodes with each node has 2 *DOF*.

Note that for the calculation of I_{mn} in the finite element, only the nodes of the vertices of the element involved in the calculation.

Table 2 : Integrals I_{mn} and I'_{mn} in the triangle of reference for $m+n=0$ up to 10.

$m+n$	m	n	I_{mn}	I'_{mn}
0	0, 0		0.5	0.5
1	1, 0	0, 1	0.1666666666	0.0000000000
2	2, 0	0, 2	0.0833333333	0.0277777777
		1, 1	0.0416666666	-0.0138888888
3	3, 0	0, 3	0.05	0.0037037037
	2, 1	1, 2	0.0166666666	-0.0018518518
	4, 0	0, 4	0.0333333333	0.0037037037
4	3, 1	1, 3	0.0083333333	-0.0018518518
		2, 2	0.0055555555	0.0018518518
	5, 0	0, 5	0.0238095238	0.0011757789
5	4, 1	1, 4	0.0047619047	-0.0005878894
	3, 2	2, 3	0.0023809523	0.0001175778
	6, 0	0, 6	0.0178571428	0.0007593572
6	5, 1	1, 5	0.0029761904	-0.0003796786
	4, 2	2, 4	0.0011904761	0.0002596511
		3, 3	0.0008928571	-0.0001996374
7	7, 0	0, 7	0.0138888888	0.0003429355
	6, 1	1, 7	0.0019841269	-0.0001714677
	5, 2	2, 5	0.0006613756	0.0000734861
	4, 3	3, 4	0.0003968253	-0.0000244953
8	8, 0	0, 8	0.0111111111	0.0001981405
	7, 1	1, 7	0.0013888888	-0.0000990702
	6, 2	2, 6	0.0003968253	0.0000560672
	5, 3	3, 5	0.0001984126	-0.0000345657
	4, 4	0.0001587301	0.0000302654	
9	9, 0	0, 9	0.0090909090	0.0001034579
	8, 1	1, 8	0.0010101010	-0.0000517289
	7, 2	2, 7	0.0002525252	0.0000251716
	6, 3	3, 6	0.0001082251	-0.0000118930
	5, 4	4, 5	0.0000721500	0.0000032000
10	10, 0	0, 10	0.0075757575	0.0000588879
	9, 1	1, 9	0.0007575757	-0.0000294439
	8, 2	2, 8	0.0001683501	0.0000154725
	7, 3	3, 7	0.0000631313	-0.0000084867
	6, 4	4, 6	0.0000360750	0.0000054929
	5, 5	0.0000300625	-0.0000044949	

To calculate I'_{mn} for the section, we must first determine the position of the center of gravity of the section to allow the use of the relations (10), because of the existence of x_G and y_G in this formula. Note that the $I_{00}=I'_{00}$ since this value represents the area of the triangle. $I'_{01}=I'_{10}=0.0$. This result giving the static moments which must be zero, since compared to the central axes, the static moments are zero. Note that the I_{10}/I_{00} represents the x_G position of the center of

gravity. Likewise for the I_{01}/I_{00} represents the value of y_G of the section. If we compare the values of I_{20} , I_{11} , I_{02} , I'_{20} , I'_{11} and I'_{01} determined by our program with those presented in (Zebbiche, Boun-jad and Allali, 2014), we find that they are the same results. This shows that our results are compared and validated. When $m+n>2$ is the goal of our work, we can say that the I_{mn} and I'_{mn} are indirectly validated since the same program carried out in the context of our work gave all the results found which is itself compared with that of (Zebbiche, Boun-jad and Allali, 2014) when $m+n=0, 1$ and 2 only, since the role of (Zebbiche, Boun-jad and Allali, 2014) is to determine the uniquely geometric characteristics of complex plane sections. We can even notice again between the values of table 2, that the $I'_{mn}<I_{mn}$ whatever the values of m and n . This result can be validated directly with the geometric characteristics. The values of I_{mn} , I'_{mn} and I'^{θ}_{mn} are always positive when m and n are both positive at the same times. While it can be positive or negative when m and n are one of the two an odd number depe.

Square Element of Reference

Figure 6 shows the square element of reference. It can be obtained from a quadrilateral element by geometric transformation. In the *FEM* quadrilateral element applications, it is sometimes recommended to work with this type of finite element instead of the quadrilateral element (Reddy, 2007) and (Imbert, 1991).

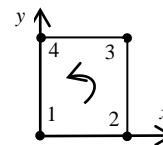


Fig. 6 Square element of reference.

For this element we have, $(x_1, y_1)=(0, 0)$, $(x_2, y_2)=(1, 0)$, $(x_3, y_3)=(1, 1)$ and $(x_4, y_4)=(0, 1)$.

To determine the results of I_{mn} and I'_{mn} for the reference square element of the figure 6 using relations (6) and (10), it suffices that to decompose the square according to two triangles 123 and 134 or according to the triangles 124 and 234.

We can show for the square of reference of figure 6 that:

$$I_{mn} = \frac{1}{(m+1)(n+1)} \tag{74}$$

And

$$I'_{mn} = \frac{[1+(-1)^m][1+(-1)^n]}{(m+1)(n+1)2^{m+n+2}} \tag{75}$$

We can use relations (74) and (75) to validate the results found by our numerical calculation program.

Table 3 shows the results of I_{mn} and I'_{mn} for the square reference element according to the figure 6

when $m+n=0$ up to 10. Note that for the calculation of I_{mn} and I'_{mn} in the finite element, only the nodes of the vertices of the element involved in the calculation.

Table 3 shows again the values of the integrals I_{mn} and I'_{mn} when $m+n=0, 1, 2, \dots, 10$ of the reference square. To calculate I'_{mn} for the square, we must first determine the position of the center of gravity of the section to allow the use of the relations (10) because of the existence of x_G and y_G in this formula. Here $x_G=y_G=0.5$. Note that the $I_{00}=I'_{00}$ since this value represents the area of the square. $I'_{01}=I'_{10}$. This result giving the static moments. Note that the I_{10}/I_{00} represents the x_G position of the center of gravity. Likewise for the I_{01}/I_{00} represents the value of y_G of the section. We can even notice again between the values of the table 3 that $I'_{mn}<I_{mn}$ whatever the values of m and n . This result can be validated directly with the geometric characteristics.

Table 3 : I_{mn} and I'_{mn} integrals in a reference square for $m+n = 0$ up to 10.

$m+n$	m	n	I_{mn}	I'_{mn}
0	0, 0		1.0	1.0
1	1, 0	0, 1	0.5	0.0
2	2, 0	0, 2	0.3333333333	0.0833333333
		1, 1	0.25	0.0
3	3, 0	0, 3	0.25	0.0
	2, 1	1, 2	0.1666666666	0.0
4	4, 0	0, 4	0.2	0.0125
	3, 1	1, 3	0.125	0.0
5		2, 2	0.1111111111	0.0069444444
	5, 0	0, 5	0.1666666666	0.0
6	4, 1	1, 4	0.1	0.0
	3, 2	2, 3	0.0833333333	0.0
7	6, 0	0, 6	0.1428571428	0.0022321428
	5, 1	1, 5	0.0833333333	0.0
8	4, 2	2, 4	0.0666666666	0.0010416666
		3, 3	0.0625	0.0
9	7, 0	0, 7	0.125	0.0
	6, 1	1, 7	0.0714285714	0.0
10	5, 2	2, 5	0.0555555555	0.0
	4, 3	3, 4	0.05	0.0
11	8, 0	0, 8	0.1111111111	0.0004340277
	7, 1	1, 7	0.0625	0.0
12	6, 2	2, 6	0.0476190476	0.0001860119
	5, 3	3, 5	0.0416666666	0.0
13		4, 4	0.04	0.0001562500
	9, 0	0, 9	0.1	0.0
14	8, 1	1, 8	0.0555555555	0.0
	7, 2	2, 7	0.0416666666	0.0
15	6, 3	3, 6	0.0357142857	0.0
	5, 4	4, 5	0.0333333333	0.0
16	10, 0	0, 10	0.0909090909	0.0000887784
	9, 1	1, 9	0.05	0.0
17	8, 2	2, 8	0.0370370370	0.0000361689
	7, 3	3, 7	0.03125	0.0
18	6, 4	4, 6	0.0285714285	0.0000279017
		5, 5	0.0277777777	0.0

Airfoils Sections

The values of the integrals I_{mn} ($m+n=0, 1, 2, \dots, 10$) in the surface of the airfoils RAE 2822 are presented in the following table 4. The reference mark for the definition of the airfoils is placed at the leading edge of the airfoil.

We notice from the table 4 that the $I_{00}=I'_{00}$ since it represents the area of the surface of the section which is an unchanged value if we change the coordinate axes. We notice from these tables that the $I'_{01}=I'_{10}=0.0$ because these axes pass through the center of gravity, and these values represent the central static moments which are zero. Note that the more $m+n$ increases, the values of I_{mn} and I'_{mn} decrease. For comparison, we notice again that $I_{00}, I_{01}, I_{10}, I_{20}, I_{02}$ and I_{11} of the RAE2822 can be found as validation in (Zebbiche, Boun-jad and Allali, 2014) as the geometrics characteristics of RAE2822.

Table 4 : I_{mn} and I'_{mn} integrals in the RAE 2822 airfoil area for $m+n=0$ up to 10.

m	n	I_{mn}	I'_{mn}
0	0	0.0778744041363284	0.0778744041363284
1	0	0.0329427779475299	0.0000000000000000
0	1	0.000346065368372	0.0000000000000000
2	0	0.0177457733254940	0.0038101723929915
1	1	0.0002198818369773	0.0000734876492881
0	2	0.0000671997163364	0.0000656618380424
3	0	0.0109040992147421	0.0001736107364692
2	1	0.0001458268516660	0.0000047923831644
1	2	0.0000272180139223	-0.0000018622524903
0	3	0.0000006951558385	-0.0000001870609197
4	0	0.0072938540664551	0.0004153410200877
3	1	0.0001005461836900	0.0000065558676835
2	2	0.0000129732186173	0.0000018529783236
1	3	0.0000003920104049	0.0000001184156901
0	4	0.0000001230557567	0.0000001185702879
5	0	0.0051799591609811	0.0000515555799315
4	1	0.0000716851639738	0.0000007812233759
3	2	0.0000069089581111	-0.0000000917632676
2	3	0.0000002305602650	-0.0000000020234031
1	4	0.0000000496664558	-0.0000000042991863
0	5	0.0000000018338643	-0.0000000008215220
6	0	0.0038466160433347	0.0000615796236919
5	1	0.0000526021932316	0.0000008046081249
4	2	0.0000039947590444	0.0000001286121619
3	3	0.0000001409121178	0.0000000069610069
2	4	0.0000000226280278	0.0000000024418076
1	5	0.000000009677828	0.0000000002656450
0	6	0.0000000002869650	0.0000000002736899
7	0	0.0029569808251991	0.0000131748064371
6	1	0.0000395731117678	0.0000001393516188
5	2	0.0000024623528670	-0.0000000047104050
4	3	0.0000000891276785	0.0000000000054388
3	4	0.0000000112941423	-0.0000000001896590
2	5	0.0000000005313315	-0.0000000000147888
1	6	0.0000000001162444	-0.0000000000111559
0	7	0.0000000000054188	-0.0000000000031182
8	0	0.0023366433184029	0.0000110019032993
7	1	0.0000304233301218	0.0000001176345058
6	2	0.0000015976813007	0.0000000126044291

5	3	0.0000000581324185	0.0000000006043373
4	4	0.0000000060593366	0.0000000001300340
3	5	0.0000000003024011	0.0000000000117389
2	6	0.0000000000518632	0.0000000000045306
1	7	0.0000000000027404	0.0000000000006966
0	8	0.0000000000007567	0.0000000000007170
<hr/>			
9	0	0.0018884356768080	0.0000032886729415
8	1	0.0000238362709238	0.0000000266225507
7	2	0.0000010811391235	0.0000000000046058
6	3	0.0000000389779112	0.0000000000167479
5	4	0.0000000034482385	-0.0000000000117254
4	5	0.0000000001778125	-0.000000000007147
3	6	0.0000000000249904	-0.000000000004138
2	7	0.0000000000014379	-0.000000000000532
1	8	0.0000000000003081	-0.000000000000317
0	9	0.0000000000000170	-0.0000000000000114
<hr/>			
10	0	0.0015549769140541	0.0000022382424625
9	1	0.0000189887214469	0.0000000192614317
8	2	0.0000007576481067	0.0000000015143298
7	3	0.0000000267939242	0.0000000000654420
6	4	0.0000000020610722	0.0000000000100520
5	5	0.0000000001077055	0.0000000000007954
4	6	0.0000000000128290	0.0000000000001985
3	7	0.0000000000007803	0.0000000000000248
2	8	0.0000000000001360	0.0000000000000100
1	9	0.0000000000000083	0.0000000000000020
0	10	0.0000000000000021	0.0000000000000019

Figures 7, 8, 9, 10 and 11 shows some examples of the generation of a structured triangular mesh in an airfoil. The example chosen is the airfoil RAE 2822. In these figures we have changed the number of points on the boundary in order to see the mesh refinement which will necessarily influence the accuracy of the obtained results.

Note that the numbering of the nodes on the upper surface begins from the trailing edge to the leading edge whereas for the lower surface, the numbering of the nodes starts from the leading edge to the trailing edge. The mesh is made so that there is condensation of nodes to the edge for rounding the bend. This procedure is especially important for subsonic and transonic airfoils.



Fig. 7 Triangular mesh in the surface of RAE 2822 airfoil with $NT=10$.

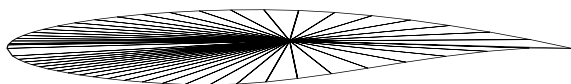


Fig. 8 Triangular mesh in the surface of RAE 2822 airfoil with $NT=50$.

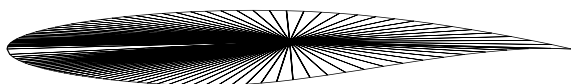


Fig. 9 Triangular mesh in the surface of RAE 2822 airfoil with $NT=100$.

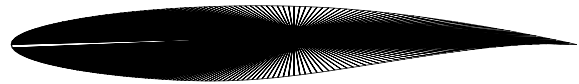


Fig. 10 Triangular mesh in the surface of RAE 2822 airfoil with $NT=300$.



Fig. 11 Triangular mesh in the surface of RAE 2822 airfoil with $NT=800$.

For example, for the following figure 12, the interior point inside is not visible in the last segment of the lower surface adjacent to the trailing edge. While this configuration is no longer valid for the calculation of I_{mn} and I'_{mn} .

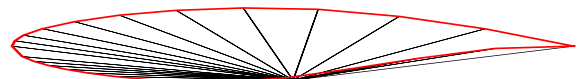


Fig. 12 Position of the internal point where it is no longer visible to the last segment of the lower surface.

Figure 13 shows some examples of structured triangular mesh generation with a single internal point in different arbitrary and complex sections used for the calculation of the integrals I_{mn} and I'_{mn} . Note that changing the internal point position does not affect the accuracy of the results. The only condition for the internal point is that it must be visible for all points of the boundary. This mesh generation step is very important for our calculation.

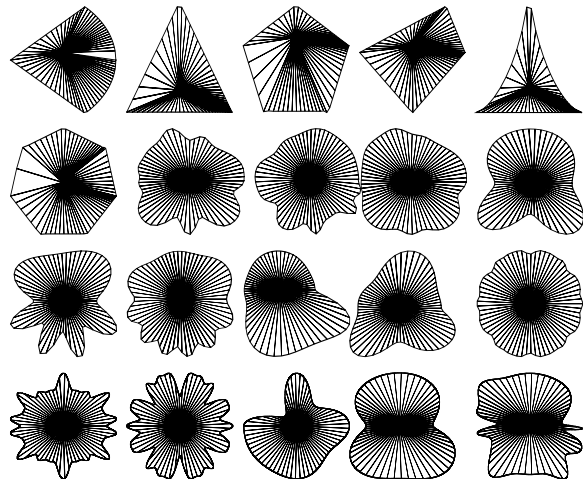


Fig. 13 Triangular mesh in selected arbitrary cross sections

Table 5 shows the effect of discretization justified by the number of triangles inside the surface of the RAE 2822 airfoil on the values of the stability coefficients as well as their quadratic moments. We clearly notice the convergence of the results with the increase in the number of triangles in order to accurately bilayer the surface of the airfoil.

Table 5 : Effect of discretization on the values of β_x' , β_y' , γ_x' , $\gamma_x'y'$, γ_y' for the airfoil RAE 2822 when NP of the Simpson's quadrature equal to 1000.

NT	$\beta_x' \times 10^6$	$\beta_y' \times 10^4$	$\gamma_x' \times 10^4$	$\gamma_x'y' \times 10^6$	$\gamma_y' \times 10^6$
10	-0.80923	-1.57308	3.38471	5.77313	1.55594
50	-4.38960	-1.74683	4.06115	6.51162	1.95627
100	-4.54340	-1.73101	4.12837	6.61229	1.96843
300	-4.59625	-1.72051	4.16311	6.66240	1.97139
500	-4.60079	-1.71926	4.16685	6.66774	1.97156
10^3	-4.60408	-1.71800	4.17049	6.67243	1.97156
3000	-4.60520	-1.71753	4.17180	6.67410	1.97154
6000	-4.60529	-1.71749	4.17190	6.67423	1.97154
10^4	-4.60531	-1.71748	4.17192	6.67426	1.97154
2×10^4	-4.60531	-1.71748	4.17193	6.67427	1.97154
3×10^4	-4.60532	-1.71748	4.17193	6.67428	1.97154
5×10^4	-4.60532	-1.71748	4.17193	6.67428	1.97154
10^5	-4.60532	-1.71748	4.17194	6.67428	1.97154

Figures 14, 15, 16, 17, 18, 19, 20, 21 and 22 represent the variation of I^{θ}_{mn} with the angle θ for the airfoil RAE 2822 when $m+n=2$ up to $m+n=10$. Note that each figure contains $m+n+1$ graphs when $m+n$ is given. In the same figure, we have grouped together the presentation of I^{θ}_{mn} and I^{θ}_{nm} .

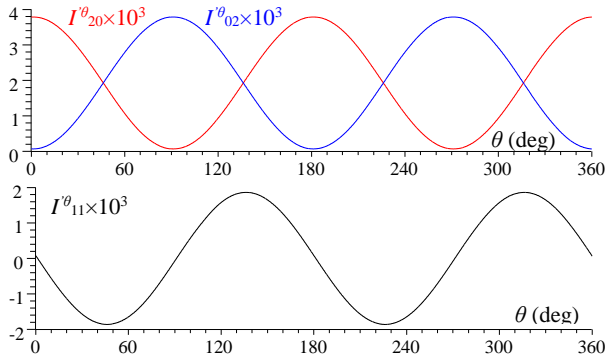


Fig. 14 Variation of I^{θ}_{mn} with θ when $m+n=2$ for the RAE 2822 airfoil.

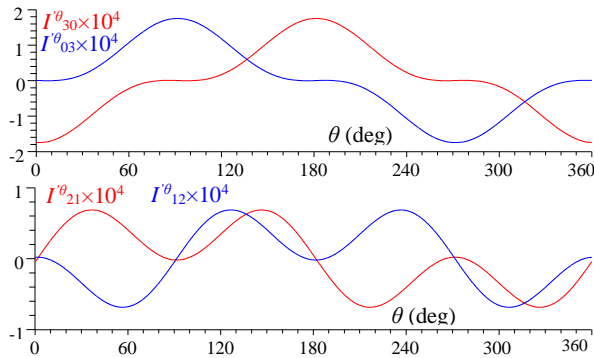


Fig. 15 Variation of I^{θ}_{mn} with θ when $m+n=3$ for the RAE 2822 airfoil.

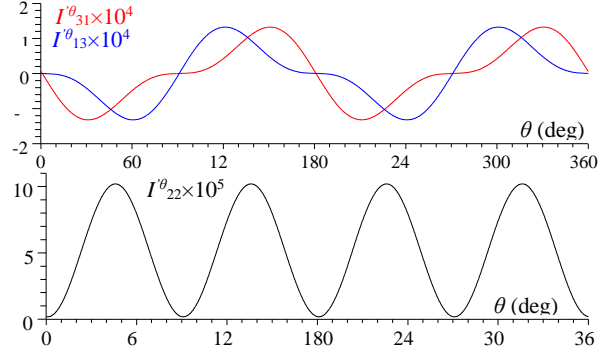
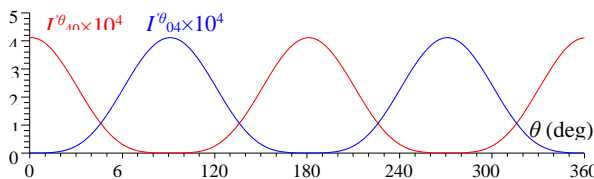


Fig. 16 Variation of I^{θ}_{mn} with θ when $m+n=4$ for the RAE 2822 airfoil.

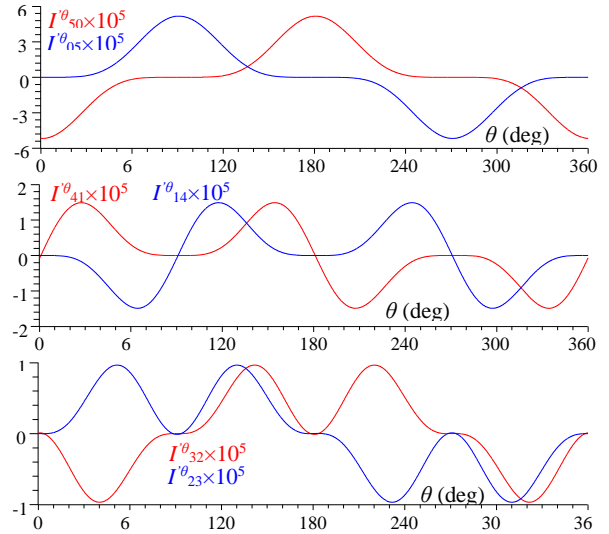


Fig. 17 Variation of I^{θ}_{mn} with θ when $m+n=5$ for the RAE 2822 airfoil.

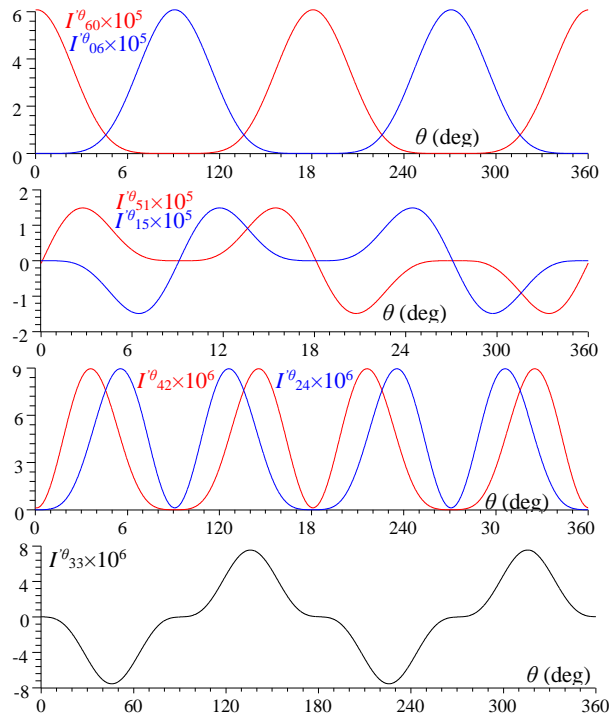


Fig. 18 Variation of I^{θ}_{mn} with θ when $m+n=6$ for the RAE 2822 airfoil.

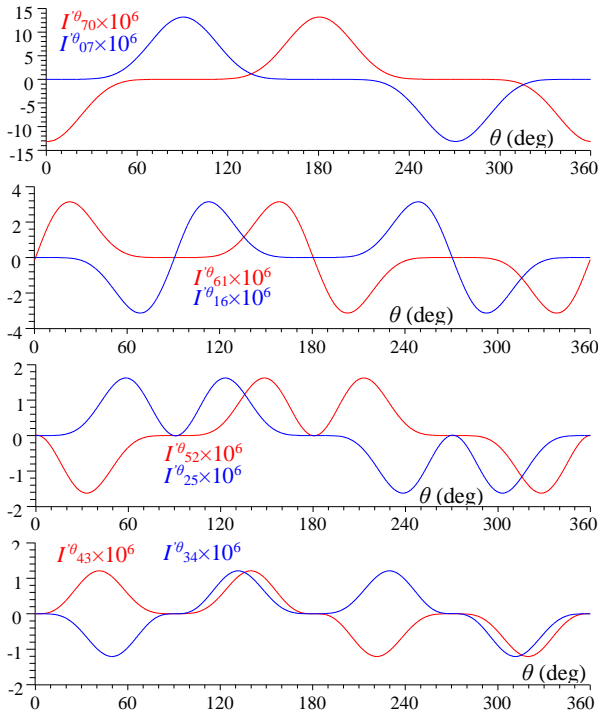


Fig. 19 Variation of I^{θ}_{mn} with θ when $m+n=7$ for the RAE 2822 airfoil.

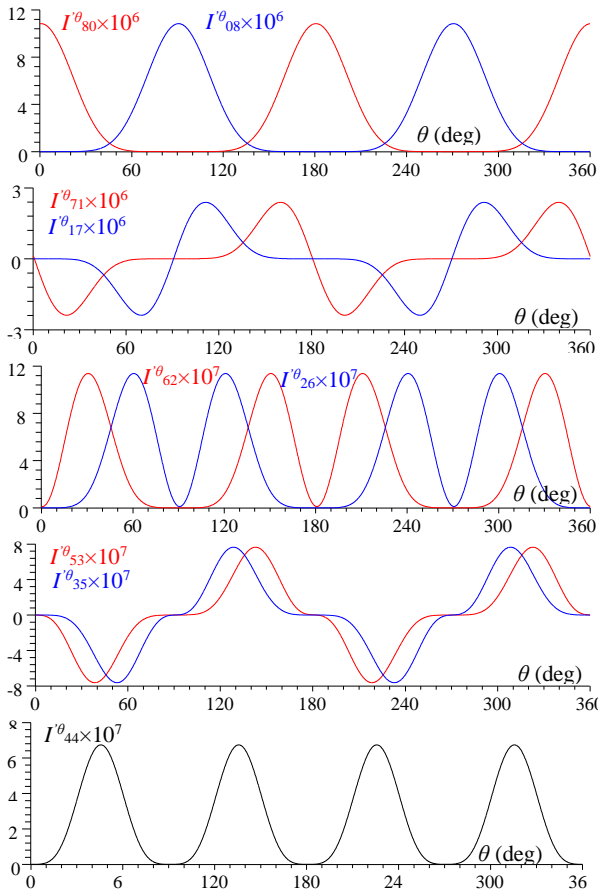


Fig. 20 Variation of I^{θ}_{mn} with θ when $m+n=8$ for the RAE 2822 airfoil.

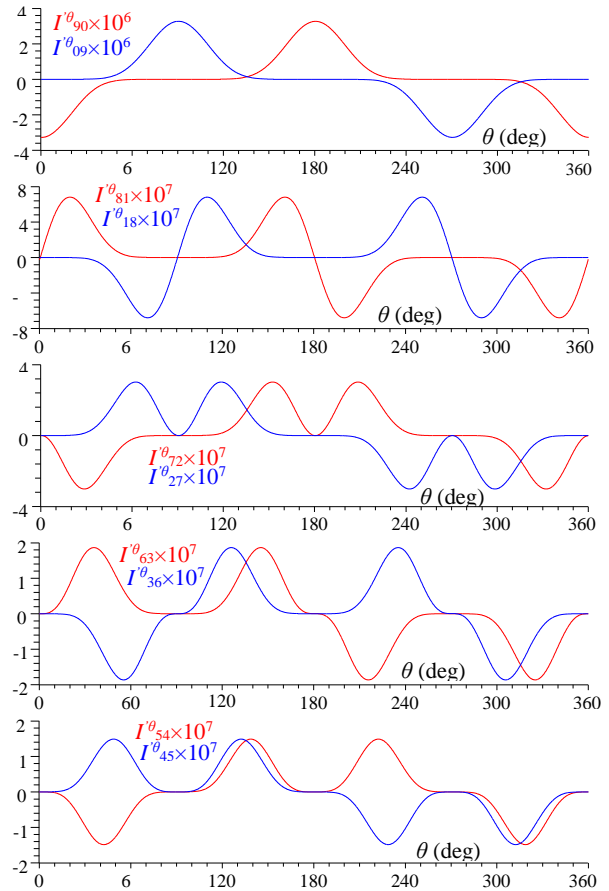
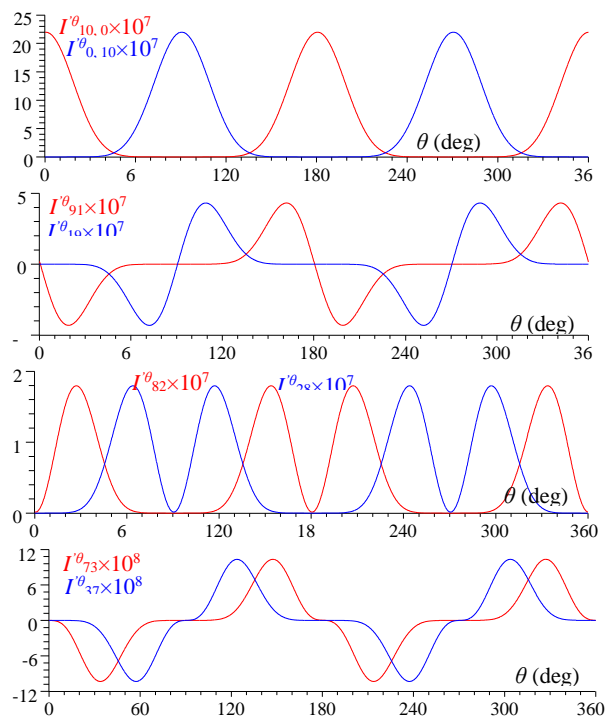


Fig. 21 Variation of I^{θ}_{mn} with θ when $m+n=9$ for the RAE 2822 airfoil.



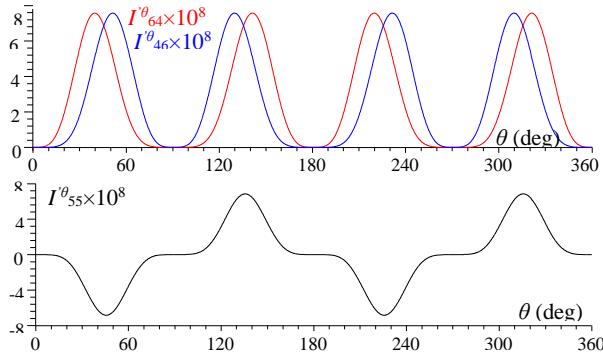


Fig. 22 Variation of I^{θ}_{mn} with θ when $m+n=10$ for the RAE 2822 airfoil.

Figure 23 represents the variation of the stability coefficients $\beta^{\theta}_u, \beta^{\theta}_v$ with θ for the airfoil RAE 2822. Note that when β^{θ}_u is zero, the other coefficient will be extreme. The values of the extremes as well as the corresponding angle are presented in table 6.

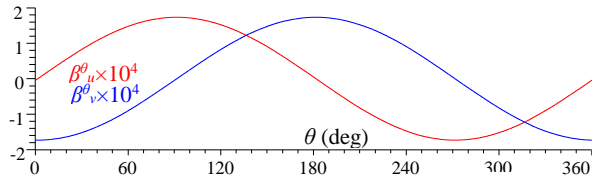


Fig. 23 Variation of the coefficients β with θ for the RAE 2822 airfoil.

Table 6 : Directions of principal axes and principal values of β for the airfoil RAE 2822.

θ (deg)	β^{θ}_u	β^{θ}_v
1.53599	0.0	-0.0001718102273460
181.53598	0.0	0.0001718102273460
91.53598	0.0001718102273460	0.0
271.53598	-0.0001718102273460	0.0

Figure 24 shows the variation of the quadratic moments of the stability coefficients. The principal directions as well as the associated values of the principal values of the moments for the airfoil RAE 2822 are represented in table 7.

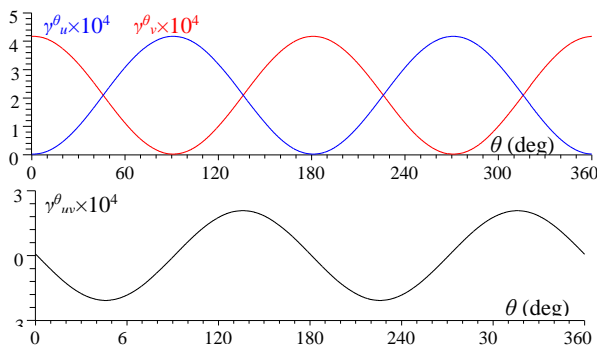


Fig. 24 Variation of the γ coefficients with θ for the RAE 2822 airfoil.

Table 7 : Directions of principal axes and principal values of γ for the airfoil RAE 2822.

θ_1 (deg)	θ_2 (deg)	$\gamma^{\theta}_u \times 10^3$	γ^{θ}_{uv}	$\gamma^{\theta}_v \times 10^3$
0.9206	180.9206	0.4173011	0.0	0.0018642
90.9206	270.9206	0.0018642	0.0	0.4173011

On the table 8, we have presented the names of the sections for which the stability coefficients as well as the quadratic moments are referenced in the table 9. In table 8, these international names represent a series of 35 airfoils according to (Suenaga and Sukai, 2001), (Abbott and Duenhoff, 1959) and (UICC Applied Aerodynamics Group, 2020). For the RAE 2822 airfoil, the results for the section 3 in table 9 also represent the results presented in the table 5 at convergence.

Table 8. Reference name of airfoils.

N	Airfoil name	N	Airfoil name
1	NACA0012	2	NACA 63-412
3	RAE 2822	4	NACA 0010-34
5	NACA 62	6	RAF 30
7	E-385	8	DOUGLAS LA203A
9	NACA 2412	10	NASA AMES A-01
11	AQUILA 9.3%	12	AVISTAR
13	CHEN	14	FAUVEL 14%
15	EIFFEL 371	16	WORTMANN FX 2
17	NACA M1	18	ONERA OA209
19	OAF 128	20	TRAINER 60
21	TSAGI 8%	22	CLARK Y-20%
23	EPPLER 520	24	NLR-7223-43
25	TH 25816 HALE	26	NYU GRUMMAN K-2
27	MVA-123	28	LISSAMAN 7769
29	GIII BL288	30	GOE 400
31	NASA LANGLEY RC-08 B3		
32	BOEING 737 OUTBOARD		
33	LOCKHEED L-188 ROOT		
34	HUGHES HELICOPTERS HH-02		
35	MARSKE PIONEER IID ROOT		

Table 9. Stability coefficients and its quadratic moments of some airfoils.

N	$\beta_x \times 10^6$	$\beta_y \times 10^4$	$\gamma_x \times 10^4$	$\gamma_{xy} \times 10^6$	$\gamma_y \times 10^6$
1	0.00000	-2.80797	5.35399	0.00000	2.44568
2	12.63056	-1.85692	3.80096	1.86923	1.86337
3	-0.46053	1.71748	4.17193	6.67427	1.97154
4	10.35767	-1.13156	4.35686	0.19361	1.46758
5	0.00000	-2.82480	4.91288	0.00000	2.39064
6	0.00000	-2.72455	5.14844	0.00000	2.56558
7	29.92404	-1.84108	2.86751	0.11724	1.44061
8	51.53089	-2.48168	5.15733	6.32306	5.92950
9	20.08276	-2.77742	5.27727	-1.23699	2.65446
10	12.29380	-2.19598	4.98200	-6.28387	1.93651
11	30.31588	-2.08618	3.74593	-7.32109	1.64671
12	31.79050	-2.95775	6.46359	-4.27312	4.50744
13	84.77736	-4.28036	6.08168	-36.04668	7.02209
14	30.28703	-3.80998	5.40173	-18.85867	4.07449
15	34.12947	-2.88466	6.21007	-14.35403	4.97590
16	21.32062	-1.13221	7.11206	17.16590	11.7670
17	0.00000	-1.34479	3.05833	0.00000	0.35709
18	6.87022	-1.61082	3.92480	-5.38042	1.24283
19	8.73461	-4.19803	5.03289	-0.85680	2.20178

20	1.69687	-5.27674	7.72399	-2.28362	7.45745
21	10.76000	-1.53823	3.49920	3.99381	0.79393
22	120.8811	-4.28812	8.66276	-60.18726	19.1903
23	-0.00140	-2.17907	4.85616	0.00053	3.78815
24	1.69955	-1.40688	3.56699	-0.06819	0.90911
25	53.54180	-1.14371	10.37429	12.85410	27.6402
26	-13.5230	-1.19692	4.179546	12.33950	2.05885
27	35.09513	-1.17905	3.06746	-7.83241	1.46373
28	36.95738	-2.95207	3.28837	-9.50243	1.98130
29	7.75857	-1.20873	3.56426	-2.82012	0.85621
30	28.44855	-2.20973	2.77190	4.63784	1.00772
31	9.59651	-1.10197	3.97635	3.03093	0.92276
32	9.36535	-1.42227	4.16141	-4.48555	1.51303
33	21.40201	-2.22891	6.10109	1.22485	4.04769
34	15.74802	-1.87201	2.89123	-3.96409	1.08199
35	15.60117	-2.96756	5.38952	-18.63651	3.42016

The present method developed for the computation of I_{mn} is a very fast method since it uses computer computation. The calculation time by computer depends on the number of triangles used in the mesh generation step as well as on the number of points used in the Simpson quadrature, without forgetting the order of calculation of $m+n$. In comparison with the old methods like the analytical method (Eiden, 2009), (Mercier, 2014), (Piskonov, 1987) and (Zebbiche, Boun-jad and Allali, 2014), we can compare the two methods to say that our method is very fast in more it can solve the problems that the old methods cannot solve them.

CONCLUSIONS

This work enabled us to develop an algorithm making fast calculation of the I_{mn} triangular integral and its applications for the calculation of the stabilities coefficients and for *FEM* elementary stiffness and mass matrices. The following conclusions are obtained:

1. Mesh generation is an essential procedure for the evaluation of I_{mn} integrals and their applications in any section.
2. Cubic spline interpolation is an essential phase for complex sections whose boundaries are given by tabulated values.
3. Simpson's quadrature is used for the numerically evaluation of the curvilinear integral of I_{mn} .
4. Green's transformation is used to go from a double integral to a curvilinear integral along the triangle boundary.
5. The position of the internal mesh point must be visible for all the nodes of the boundary.
6. The increase in the number of nodes on the boundary is necessary to have a convergence.
7. The coefficients of stabilities as well as their quadratic moments are particular cases of the computation of I_{mn} respectively when $m+n=3$ and $m+n=4$.
8. The program developed to do the numerical calculation of I_{mn} of a reference triangle as well

as for any section of arbitrary complex geometries. Like arbitrary triangles and quadrilateral.

9. The numerical program to do the calculation of I_{mn} for which value of $m+n$. The application is made for $m+n=0$ up to 10.
10. For the elementary applications in *FEM*, only the nodes of the vertices of the triangle intervening in the computation of I_{mn} .
11. One can consequently develop matrices of rigidities and masses of the finite elements possessing numbers of high *DOF*.
12. Two methods, one analytical and the other numerical are presented for the evaluation of the integral I_{mn} .
13. The work presented can be used for all disciplines that use the *FEM*. Especially the engineering.
14. To go from I_{mn} to I'_{mn} , it is necessary to first evaluate the values of x_G and y_G of the section.
15. The computation of the geometrical characteristics when $m+n=0, 1$ and 2 are a particular case of our work.
16. Our work is specially designed for the evaluation of I_{mn} when $m+n>2$.

As perspectives, we can extend the work in order to determine the elementary stiffness and mass matrices of triangular finite elements having a very large number of nodes or *DOFs* by using our work of calculating I_{mn} .

The second work consists in making an extension to determine the integrals I_{mn} and in particular the stability coefficients of doubly and multi-connected complex sections.

REFERENCES

- Abbott I. H. and von Doenhoff A. E., "Theory of wing sections: Including a summary of Airfoil data," Dover Publications, Inc., New York, Vol. II, (1959).
- Démidovitch B. and Maron I. "Eléments de calcul numérique," Editions MIR, Moscow, Russia, (1987).
- Eiden J. D., "Géométrie analytique classique," Edition Calvage et Mounet, 1ère Edition, France, (2009).
- Imbert J. F., "Analyse des Structures par Eléments Finis," 3^{ème} Edition, Sup'Aéro, Cepadues-Editions, France, (1991).
- Irons B. and Ahmed S., "Techniques of Finite Elements," John Wiley and Sons., New York, (1990).
- Kardestuncer H. et al, "Finite Element Handbook," McGraw-Hill Book Company, USA, (2010).

Ladson, C., Brooks, C., "Development of a Computer Program to obtain Ordinates for NACA 4-Digit, 4-Digit Modified, 5-Digit, and 16-Series Airfoils," NASA TM X-3284, (1975).

Lehning H., "Toutes les mathématiques du monde," Flammarion, France (2017).

Lofficial M. and Tanré D., "Intégrales curvilignes et de surfaces," Edition Ellipses, Paris, France, (2006).

Megson T. H. G., "Structures and Stress Analysis," 2nd edition, Elsevier, Oxford, (2005).

Megson T. H. G., "Aircraft Structures for Engineering Students," 4th edition, Elsevier, Oxford, (2007).

Mercier D. J., "Cours de géométrie," Create Space Independent Publishing Platform; 4e édition, France, (2014).

Piskounov N., "Calcul différentiel et intégral," tome 2, Edition Mir, Moscow, URSS, (1987).

Ralston A. and Rabinowitz A., "A First Course in Numerical Analysis," McGraw Hill Book Company, (1985).

Reddy J. N., "An Introduction to the Finite Element Method," Edition Mc-Graw Hill Book Company, (2007).

Suenaga K. and Sakai M., "A cubic spline approximation of an offset curve of a planar cubic spline," International Journal of Computer Mathematics, Vol. 78, N° 03, PP. 445-450, (2001), <https://doi.org/10.1080/00207160108805122>.

UIUC Applied Aerodynamics Group, department of Aerospace Engineering, College of Engineering, University of Illinois at Urbana, Champaign, Il, (2020), http://www.ae.illinois.edu/mseelig/ads/coord_database.html

Zebbiche T., Boun-jad M. and Allali A., "Structural characteristics of simply connected planar sections with application to airfoils," Journal of Materials and Engineering Structures, Vol. 1, N° 02, PP. 89-98, September (2014).

NOMENCLATURE

I_{mn}	Integral with respect to the reference mark of the definition axes of the section.
I'_{mn}	Integral with respect to the reference mark of the central axes.
J_{12}, J_{23}, J_{31}	Integral along the three sides of the triangle in the Oxy coordinate system.
$J'_{12}, J'_{23}, J'_{31}$	Integral along the three sides of the triangle in the $Gx'y'$ coordinate system.
m, n	Order of x and y in I_{mn} integral.

(x, y)	Cartesian abscissa and ordinate of a node.
z	Integral variable.
N	Number of points on the boundary of the section.
NT	Number of triangles in the section.
NP	Number of points of the Simpson quadrature.
P	Internal point (Observer).
Δ	Triangular element Area.
F, G	Functions used for the Green Transformation.
β	Stability coefficients.
θ	Central axes angle of rotation.
A	Area of the section.
Ox, Oy	Reference definiton axes of the section.
Gx', Gy'	Central axes of the section.
$[K]^e$	Elementary stiffness matrix.
$[M]^e$	Elementary mass matrix.
$[E]$	Young Matrix.
DOF	Degree Of Freedom.
FEM	Finite Elements Method.
ρ	Density of the finite element.
t	Finite element thickness.
$[N]$	Interpolation functions of a finite element.
$[B]$	Matrix derived from interpolation functions.
u, v, w	Displacements functions in a finite element.
γ	Quadratic moment of the coefficient of stability.
C	Chord of airfoils.

Indice

1	Node 1.
2	Node 2.
3	Node 3.
12	Between nodes 1 and 2.
23	Between nodes 2 and 3.
31	Between nodes 3 and 1.
G	Center of gravity.
mn	Regarding integrals I_{mn}, I'_{mn} and I^{θ}_{mn} .
x	With respect to the Ox axis.
y	With respect to the Oy axis.
x'	Relative to the Gx' axis.
y'	With respect to the Gy' axis.
u	With respect to the Gu axis.
v	With respect to the Gv axis.

Exposant

θ	Compared to Guv benchmarks.
----------	-------------------------------